Augmenting Anti-Tumor T Cell Responses to Mimotope Vaccination by Boosting with Native Tumor Antigens

Jonathan D. Buhrman[1], **Kimberly R. Jordan**[1], **Lance U'Ren**[1], **Jonathan Sprague**[1], **Charles B. Kemmler**[1], and **Jill E. Slansky**[1]

[1]Integrated Department of Immunology, University of Colorado School of Medicine, Denver, CO

Abstract

Vaccination with antigens expressed by tumors is one strategy for stimulating enhanced T cell responses against tumors. However, these peptide vaccines rarely result in efficient expansion of tumor-specific T cells or responses that protect against tumor growth. Mimotopes, or peptide mimics of tumor antigens, elicit increased numbers of T cells that cross-react with the native tumor antigen, resulting in potent anti-tumor responses. Unfortunately, mimotopes may also elicit cells that do not cross-react or have low affinity for tumor antigen. We previously showed that one such mimotope of the dominant MHC class I tumor antigen of a mouse colon carcinoma cell-line stimulates a tumor-specific T cell clone and elicits antigen-specific cells *in vivo*, yet protects poorly against tumor growth. We hypothesized that boosting the mimotope vaccine with the native tumor antigen would focus the T cell response elicited by the mimotope towards high affinity, tumor-specific T cells. We show that priming T cells with the mimotope, followed by a native tumor-antigen boost improves tumor immunity, compared to T cells elicited by the same prime with a mimotope boost. Our data suggest that the improved tumor immunity results from the expansion of mimotope-elicited tumor-specific T cells that have increased avidity for the tumor antigen. The enhanced T cells are phenotypically distinct and enriched for T cell receptors previously correlated with improved anti-tumor immunity. These results suggest that incorporation of native antigen into clinical mimotope vaccine regimens may improve the efficacy of anti-tumor T cell responses.

Keywords

mimotope; T cell; affinity; vaccine; altered-peptide ligands

Introduction

Harnessing the specificity of the adaptive immune system, primarily T cells, to control tumor growth is a major focus of cancer immunotherapy. Tumors provide unique challenges towards inducing effective anti-tumor T cell responses, including tumor-induced immune suppression and tolerance towards tumor-associated antigens (TAA) (1, 2). Many TAA are dysregulated, non-mutated self-antigens and therefore the majority T cells with high avidity for TAA are purged from the thymus during negative selection (3). However, negative selection of self-specific T cells is often incomplete and some TAA-specific T cells escape the thymus and enter the periphery (4). Whether expanded by vaccines or other

immunological interventions, these remaining cells, if activated properly, may be instrumental for cancer immunotherapy (5). Although several creative strategies have been attempted, more work is needed to improve anti-tumor T cell immunity.

Vaccination with TAA typically elicits minimal expansion of tumor-specific T cells, resulting in a failure to control tumor growth (6). One approach to improve the T cell response against tumors is vaccination with peptide mimics of tumor antigens, or mimotopes (7). Mimotopes, also referred to as altered peptide ligands, analog peptides, or variant peptides, resemble tumor antigens but have amino acid substitutions that affect peptide-MHC (pMHC) or T cell receptor (TCR) interactions (7). Initially, mimotopes consisted of amino acid substitutions of MHC-anchor residues, which increased the affinity of the peptide-MHC interaction, resulting in enhanced presentation (8). While these mimotope vaccines increased the frequency of tumor-specific T cells, the T cells often recognized tumor antigens poorly and resulted in minimal tumor protection (9, 10). Current data suggest that even subtle changes in peptide sequence may dramatically alter T cell interactions and the repertoire of responding T cells resulting in the activation of T cells that do not recognize the native peptide (11–14). Therefore, mimotopes may be beneficial or inhibitory to the immune response, the results of which may be unknown prior to vaccination.

We are developing vaccination strategies using mimotopes of the immunodominant CD8+ T cell epitope, AH1 *(SPSYVYHQF)*, of the mouse colon carcinoma cell-line CT26. Utilizing a tumor-specific T cell clone, we identified mimotopes that afford a range of protection from tumor growth (7, 15–17). We demonstrated that protective mimotopes elicit more high affinity AH1 cross-reactive cells than poorly protective mimotopes (17), and that the responding T cells from protective vaccines more closely resemble the T cell repertoire responding to native AH1 (18). Thus, we hypothesized that boosting mimotope-elicited T cell responses with the native antigen, rather than the mimotope peptide, would select for T cells with increased affinity for the native antigen and improve anti-tumor immunity. Clinical studies immunizing with an altered peptide ($TERT_{572Y}$) for a cryptic epitope derived from human telomerase (hTERT) followed by boosts with the native peptide ($TERT_{572R}$) resulted in higher quality T cell responses when compared to successive immunization with the altered peptide (19–21). We tested this hypothesis with mimotope-15 *(MPKYAYHML)*, which poorly protects against tumor growth and elicits many AH1-specific T cells that do not function in response to stimulation with AH1 *ex vivo* (17). Mimotopes are essential to initially expand AH1-cross-reactive cells because immunization with native AH1 peptide does not elicit robust expansion of AH1-specific T cells or protect mice from CT26 growth (15, 17).

We show here that boosting the mimotope-15-elicited T cells with native antigen results in fewer AH1-specific cells overall, yet these T cells had increased functional avidity for the tumor antigen. This vaccine strategy elicited T cells that killed AH1-pulsed targets more efficiently, produced more IFNγ and TNFα following stimulation with AH1 peptide, and improved anti-tumor immunity. *Ex vivo* analysis of these T cell clonotypes revealed that the dominant TCRβ chains are shared with those from the mimotope-15 vaccine, although at higher frequency. While immunization with the native AH1 antigen in the absence of the mimotope-prime elicited low frequencies of AH1-specific cells, the cells that did respond are high-quality cells and their deficiency in tumor protection may be attributed to their inability to expand sufficiently. These results demonstrate that mimotope vaccines expand a broad repertoire of T cells with a range of affinity for the tumor antigen and a subsequent boost with the native antigen selects for T cells with increased functional recognition of the tumor. This simple concept could be readily incorporated into current trials using mimotope vaccines and may potentially improve the quantity and quality of tumor-specific T cells.

Materials and Methods

Mice

Six- to 8-week-old female BALB/cAnNCr mice were purchased from the National Cancer Institute/Charles River Laboratories. *Gp70*$^{-/-}$ mice were produced by selective breeding as described (22). All animal protocols were reviewed and approved by the Institutional Animal Care and Use Committee at National Jewish Health.

Cells

Sf9 and High Five insect cells (Invitrogen) and CT26 tumor cells were cultured as described (16). CT26 tumor cells are progeny of cells purchased from ATCC in 1996. CT26 expression of the gp70 protein from the endogenous ecotropic murine leukemia virus was verified by flow cytometry as described (23).

Peptides

Recombinant baculoviruses (BV) were engineered and produced as described (24). Soluble synthetic peptides were   95% pure (Chi Scientific).

Vaccines

Mice were primed with 10^7 recombinant-BV infected Sf9 insect cells as described (16). Mice were boosted 7 days later with 100 μg of the indicated peptide, 50 μg agonistic anti-CD40 antibody (F6K4.5; BioXcel), and 50 μg Poly:IC (Amersham) intraperitoneally. 15–15 refers to mice primed with mimotope-15 and boosted with mimotope-15. 15-AH1 refers to mice primed with mimotope-15 and boosted with the AH1 peptide.

H-2L^d tetramer staining

R-PE-conjugated H-2L^d-tetramers were produced in house as described (15). Dual tetramer staining was performed using covalently linked peptide H-2L^d tetramers as described (17). Splenocytes were incubated at room temperature for 90 min with peptide-loaded tetramer, FcR antibody (2.4G2), viability-discriminating agent 7-aminoactinocycin D (7-AAD; Sigma), and fluorochrome-conjugated Abs (Biolegend) against CD8 (53–6.7), CD11a (M17/4), CD4 (RM4-5), B220 (RA3-6B2), and I-A/I-E (M5/114.15.2). CD4/B220/I-A/I-E antibodies and 7-AAD are collectively referred to as the 'Dump' gate. Where indicated cells were stained with antibody against PD-1 (29F.1A12), KLRG-1 (2F1/KLRG), and IL-7Rα (A7R34). Cells were analyzed on a CyAn flow cytometer (Beckman Coulter) or FACSCalibur (BD Biosciences) and data were processed using FlowJo software (Tree Star). Tetramer dissociation assays were performed as described (18).

Intracellular cytokine staining

One week following the second vaccination, splenocytes were stimulated with the indicated peptide and GolgiStop in 96-well plates for 5 h per the manufacturers instructions (BD Cytofix/Cytoperm Plus Fixation/Permeabilization Kit, BD Pharmingen). Following cell surface staining, fixation, and permeabilization, cells were stained with antibody against mouse IFNγ (APC or PE) for 1 h at 4°C. In some experiments, antibody for TNFα (AF488) was included.

In vitro killing assay and IFNγ ELISA

Splenocytes from multiple mice were combined and CD8+ T cells were enriched using the Dynal CD8+ Negative Selection Kit (Invitrogen). AH1-tet^{hi} AH1-tet^{lo}, and AH1-tet^{neg} CD11a^{lo} cells were sorted to ~70–95% purity on the iCyt Synergy cell sorter. GP70–/–

splenocytes were isolated and labeled as target cells. Splenocytes were pulsed for 3 h in the absence of FBS with 10 μg/ml AH1, 15, or βgal-peptides. Cells were washed and labeled with either 5 μM CFSE (AH1, 15) or 0.5 μM CFSE (βgal). Equal numbers of AH1 or 15-targets were incubated with 5×10^4 sorted AH1-tet[hi] effectors. Twelve hours following incubation the cells were washed and stained with 7-AAD to exclude dead cells and the number of CFSE+7-AAD- target cells was determined. Specific killing was determined as described (17). Supernatant from killing assay was collected and IFNγ production was measured using the BD OptEIA IFNγ ELISA kit.

TCR Sequencing

Eight-10 mice were immunized as described and splenocytes combined based on the vaccine. AH1-tet+ T cells were sorted ($2–3\times10^5$), mRNA was isolated using TRIzol[®] Reagent, and first strand cDNA was generated using random hexamers and SuperScript III Reverse Transcriptase (Invitrogen). High-throughput sequencing PCR reactions were performed as described for all Vβ8 family members (with barcode identifiers for each vaccine type) (18). Amplicons presenting the expected size of 300–400 bp were quantified by fluorescent measurement using the QubiT[®] ds DNA HS assay (Invitrogen). Equimolar pools of barcoded amplicons were produced and used in an emulsion PCR. The emPCR, corresponding to clonal amplification of the purified amplicon pool, was carried out using the 454 GS FLX Titanium (Roche Diagnostics) according to the manufacturer's recommendations. Sequencing data were analyzed as described (18).

TIL isolation

Mice were vaccinated as described above. One day following the boost mice were challenged with 5×10^4 CT26 tumor cells subcutaneously and monitored until βgal-vaccinated control tumors reached ~25 mm^2. Tumors were collected and cut into small pieces, incubated with 0.1 mg/ml Liberase (Roche) for 30 min at 37°C, and large clumps were broken up by trituration with an 18 g needle. Single cell suspensions were either stained directly or stimulated with 10 μg/ml AH1-peptide for 5 h for intracellular cytokine staining.

Tumor challenge

One week following the second vaccination (day 0) mice were challenged with 5×10^4 CT26 tumor cells subcutaneously in the left hind flank (22). Tumor-free survival was assessed by palpation of the injection site and mice were sacrificed when the tumors reached 100 mm^2.

Statistical analyses

Tumor-free survival was analyzed on Kaplan-Meier survival plots and statistical significance was analyzed with Prism version 4.0, GraphPad Software, using the log-rank test. Other analyses was performed using an unpaired two-tailed Student's *t* test. A *p* value of <0.05 was considered statistically significant and error bars represent the standard error of the mean unless otherwise noted.

Results

An increased proportion of T cells elicited by vaccination with mimotope-15 followed by native AH1 boost cross-react with AH1

Vaccination with the AH1-peptide tumor antigen elicits few AH1-specific T cells and does not provide protection against subsequent CT26 challenge (17). Conversely, vaccination with mimotope-15 expands significantly more AH1-specific T cells yet only 20% of mice survive following CT26 tumor challenge (17). We previously reported that a majority of

mimotope-15 elicited T cells do not recognize AH1, and therefore, we hypothesized that we could improve anti-tumor immunity elicited by poorly protective mimotopes, such as mimotope-15, by boosting with the native AH1 peptide. Using a prime-boost protocol, we immunized initially with baculovirus-infected Sf9 insect cells expressing either mimotope-15 or the AH1 peptide and seven days later boosted this response with either of the peptides in conjunction with Poly-IC and αCD40 (16, 25). This regimen elicited more antigen-specific T cells than either insect cells or Poly:IC/αCD40 alone in the prime and boost (data not shown). Using H-2L^d tetramers loaded with AH1-peptide (AH1-tet), we determined the total number of AH1-specific cells, and the frequency, in the spleen seven days following the boost (Fig. 1A and B). Surprisingly, the number and frequency of AH1-tet+ cells in the spleen was decreased in mice boosted with the AH1 peptide. As expected, the AH1-AH1 vaccine generated very few AH1-specific cells. However, one mouse of 18 tested had a substantial response to the AH1-AH1 vaccine. If these data are analyzed using the Mann-Whitney test, or if the outlier is excluded, significant differences (p < 0.0001) between the AH1-AH1 group and either 15–15 or 15-AH1 are observed.

We next determined the frequency of T cells that cross-reacted with the AH1 peptide. We vaccinated mice as above and stained splenocytes with either AH1- or 15-loaded H-2L^d tetramer. The frequency of 15-specific cells that cross-reacted with AH1 was significantly greater following the 15-AH1 vaccination (Fig. 1C and D). Similar results were observed in experiments where cells were co-stained with covalently linked AH1 or 15-tetramers (17) conjugated to different fluorophores (Fig. 1E). Experiments using an irrelevant peptide (βgal) to prime the immune response, followed by a boost with the AH1 peptide, resulted in the detection of background levels of AH1-specific cells (data not shown), suggesting that the AH1-boost is not generating detectable AH1-specific cells in the absence of the mimotope-15 prime and that cross-reactive T cells are necessary for the response. Thus, the 15-AH1 vaccine did not increase overall cell numbers, but focused the response towards the AH1-tumor antigen.

15-AH1 vaccination elicits CD8+ T cells with greater affinity for AH1-tet than the 15–15 vaccine

While examining the AH1-specific T cells in Figure 1, we observed differences in AH1-tet+ staining intensity that warranted further analysis. The mean fluorescence intensity (MFI) of tetramer staining has been correlated with increased T cell affinity for antigen (26, 27). We observed that AH1-specific cells expanded by the AH1-boost stained more intensely with AH1-tet as determined by geometric MFI (Fig. 2A and B). Interestingly, the small frequency of AH1-specific cells elicited by the AH1-AH1 vaccine stained with similar intensity as the 15-AH1 cells, suggesting a similar avidity for AH1-tet. Importantly, co-staining with a TCR-specific antibody suggested that TCR expression was slightly lower on the AH1-boosted cells indicating that their increased staining intensity for AH1-tet was not due to increased TCR expression (data not shown). We extended this analysis by examining the kinetics of the pMHC:TCR interaction with a tetramer dissociation assay. Tetramer dissociation correlates with the off-rates of monomeric pMHC:TCR affinity as measured by surface-plasmon resonance (28). AH1-specific cells from mice boosted with the AH1 peptide had a slower rate of tetramer decay following the addition of an MHC Fab-specific competitor and significantly longer half-lives of tetramer association than those that received the 15–15 vaccine (Fig. 2C and D). Combined, these results suggest that the T cells elicited by 15-AH1 vaccination have increased avidity for the native AH1-peptide.

AH1-specific cells following 15-AH1 vaccination produce more pro-inflammatory cytokines following ex vivo stimulation

Increased pMHC:TCR interaction detected by tetramer binding does not always correlate with increased function (29). Therefore, we determined if the T cells elicited by each vaccine strategy produced cytokines upon antigen recognition. We stimulated splenocytes from vaccinated mice with increasing concentrations of AH1-peptide and measured intracellular IFNγ production. We observed an increase in the total number of IFNγ-producing cells elicited by the 15–15 vaccine at high peptide concentrations (Fig. 3A). This result was not surprising since the 15–15 vaccine elicited more total AH1-tet+ T cells (Fig. 1). The total number of IFNγ+ cells from AH1-AH1 vaccination was low, again attributed to the low number of AH1-tet+ cells that respond to this vaccine (Fig. 1). However, when IFNγ production is plotted as a frequency of AH1-tet+ cells, a greater frequency of the AH1-tet+ cells from the 15-AH1 and AH1-AH1 vaccines produced IFNγ (Fig. 3B). Thus, a greater proportion of the AH1-tet+ cells elicited by these regimens functionally recognize AH1. Consistent with the increased affinity as detected by tetramer staining (Fig. 2), the 15-AH1 vaccine elicited IFNγ producing T cells with increased sensitivity for the AH1 peptide (Fig. 3C and D). AH1-AH1 vaccination, albeit low in frequency, elicited T cells with enhanced functional avidity towards AH1. Furthermore, analyses of the geometric MFI revealed that stimulation of AH1-boosted T cells resulted in significant increases in the amount of IFNγ produced by each T cell, suggestive of a higher quality response (Fig. 3E).

Increased T cell function and quality has been correlated to not only the production of IFNγ, but also the production of other cytokines, such as TNFα and IL-2 (30). More of the IFNγ+CD8+ T cells in the AH1-boosted mice produced TNFα (Fig. 3F). However, we observed no difference in IL-2 production (data not shown). Importantly, when splenocytes were stimulated with mimotope-15 *ex vivo*, we saw no differences in cytokine production, suggesting these cells were not defective, but indeed had lower sensitivity for the AH1-peptide (data not shown). Overall, these results support the hypothesis that the 15-AH1 vaccine strategy elicits a higher quality AH1-specific T cell population than the 15–15 vaccine and the AH1-AH1 vaccination elicits very low frequencies of high-quality T cells.

15-AH1 vaccination elicits an increased frequency of 'short-lived effector' AH1-specific T cells

We next determined if the 15-AH1 vaccine altered the effector phenotype of AH1-specific T cells. KLRG-1 and IL-7Rα markers have been commonly used to identify short-lived effector cells (SLEC; KLRG-1+IL-7Rα-) or memory-precursor effector cells (MPEC; KLRG-1-IL-7Rα+) (31). SLEC are terminally differentiated T cells with immediate cytolytic effector function and increased expression of the transcription factor T-bet (32, 33). Interestingly, a greater frequency of the AH1-tet+ T cells from the 15-AH1 mice were identified as SLEC compared to cells from the 15–15 group (Fig. 4A and B). T cells from the 15–15 group also had significant increases in the frequency of MPEC and early-effector cells (EEC; KLRG-1-IL-7Rα-). The phenotype of the AH1-tet+ cells from AH1-AH1 vaccination had equal frequencies of both MPEC and SLEC, and increased IL7Rα+KLRG-1+ cells (Fig. 4 A and B). Lastly, we examined PD-1 expression on CD8+ T cells, which increases upon activation and remains high on exhausted or anergic cells (34). AH1-tet+ cells from the 15-AH1 and AH1-AH1 groups had significantly lower levels of PD-1 expression compared to homologous 15–15 vaccination (Fig. 4C and D). In combination, these results suggest that the AH1-specific cells from each vaccine may be receiving different stimuli during vaccination and therefore have different activation profiles.

The 15-AH1 vaccine stimulates T cells that more efficiently lyse AH1+ target cells

We next determined if AH1-specific cells from each group killed AH1-expressing targets cells with similar efficiency. We sorted AH1-tet+ cells from 15–15 and 15-AH1 mice (Fig. 5A) and showed that AH1-tet+ cells from the 15-AH1 mice killed more effectively than AH1-tet+ cells from 15–15 mice (Fig. 5B). Closer examination of the AH1-tet+ cells elicited from 15–15 vaccination revealed two populations of cells with different staining intensities for AH1-tet (AH1-tet^{hi} and AH1-tet^{lo}) (Fig. 5A). Only one population of AH1-tet + cells was detected after the AH1-boost (AH1-tet^{hi}). To determine if the AH1-tet^{lo} cells were inhibiting the function of AH1-tet^{hi} cells in the 15–15 group, we sorted the AH1-tet^{hi} cells from both groups and used them with and without the AH1-tet^{lo} cells in killing assays. In the absence of AH1-tet^{lo} cells, the AH1-tet^{hi} cells from the 15–15 mice were less effective than AH1-tet^{hi} from the 15-AH1 (Fig. 5B). The dysfunction in killing from 15–15 vaccine-elicited T cells was specific for AH1-loaded targets as they effectively killed mimotope-15-loaded targets (Fig. 5B). To confirm that these groups of T cells produced and secreted IFNγ as assumed in Fig. 3D, we collected supernatant from the killing assays and measured IFNγ by ELISA. As expected, the T cells from the 15-AH1 group generated more IFNγ than the other groups (Fig. 5C). Overall, these results suggest that the AH1-tet+ cells elicited by each vaccine have different phenotypes and functional reactivity towards AH1.

Heterologous AH1-boost preferentially expands a subset of T cells elicited by priming with the mimotope-15 vaccine

Previous analyses of AH1-specific cells responding to mimotope vaccines revealed a positive correlation between tumor protection and Vβ8.3-expressing TCRs paired with Jβ2.6 gene fragments (18). Increased representation of Vβ8.3+Jβ2.6+ cells was also identified in the responses to the native AH1 vaccine. Data presented above suggest that the heterologous 15-AH1 vaccine elicits high-quality T cells, similar to the cells elicited by AH1. Thus, we determined if the AH1 boost selected specific T cells elicited by the mimotope-15 prime and whether these cells were similar to those described. We pooled sorted AH1-tet+ cells from several mice, generated cDNA, and performed high throughput sequencing using Vβ8-family specific primers. Greater than 22,000 sequences per group were analyzed as described (18). The heterologous AH1-boost significantly enhanced the frequency of Vβ8.3+ clonotypes expressing Jβ2.6 compared to AH1-tet^{hi} T cells from the 15–15 group (Fig. 5D). Not surprisingly, the frequency of Vβ8.3+ sequences expressing Jβ2.6 were similar to those of the AH1-tet+ cells from AH1-AH1 vaccination. These results suggest that the robust stimulation provided by the mimotope-15 vaccine may elicit a broad repertoire of T cells and the native AH1 boost focuses the response towards T cells expressing Jβ2.6.

Another common feature identified within AH1-specific T cells identified from protective vaccines was a relatively short CDR3β length of 10 amino acids (18). Over 70% of all Vβ8.3+ sequences following the heterologous AH1 boost had a CDR3β length of 10 amino acids, while that frequency was lower in all mimotope-15 vaccine groups (Fig. 5E). Surprisingly, the majority of Vβ8.3+ sequences from the AH1-AH1 vaccine were 9 amino acids. A single dominant clone that was identified 5,350 times out of 8,188 Vβ8.3+ sequences largely influenced these results. Our previous observations also identified a motif within the CDR3β, consisting of a small hydrophobic residue, followed by a large polar residue, and the tyrosine residue unique to Jβ2.6 (18). Upon analysis of the Vβ8.3+ sequences identified within each population, the AH1-boost significantly enriched for T cells expressing this CDR3β motif (Fig. 5F, Table 1). In contrast to our previous data indicating that AH1 elicits the same motif-expressing cells (18), the AH1-specific cells elicited in this experiment did not meet the strict definition of the motif (Fig. 5F). Several differences in experimental design, including pooled T cells from multiple mice and tetramer design, may account for these differences. Additionally, the dominant clone

identified in AH1-AH1 cells was one amino acid short of the motif, dramatically impacting the results.

The majority of the CDR3β sequences identified from the heterologous AH1-boost (88.5%) were also identified in the homologous 15–15 cells, albeit at lower frequencies (Table 1). Only one sequence (light grey) from the dominant 15-AH1 clones was identified in the AH1-AH1 vaccine but not 15–15 (0.76%), suggesting that most of the AH1-specific T cells from the 15-AH1 vaccine originated from the 15-prime. Thirty percent of the dominant 15-AH1 sequences were identified in both AH1-AH1 and 15–15 groups, suggesting the possibility that either vaccine could elicit the same cell, although the frequencies are more consistent with the mimotope priming these cells.

Increased frequency of functional AH1-tet+T cells infiltrate the tumor, express less PD-1, and enhance tumor-free survival following 15-AH1 vaccination

Next we determined the difference between the vaccine groups in T cell infiltration and function within the tumor. To ensure tumor growth, we challenged mice with CT26 tumor cells immediately following the boost. When control tumors (βgal vaccinated or unvaccinated) were approximately 25 mm^2, the infiltrating CD8+ T cells, or TIL, were examined. Significant differences in the number of AH1-tet+ TIL per milligram of tumor were not observed between the two groups, although there was a trend towards more cells following 15–15 vaccination (Fig. 6A). However, similar to the periphery, we observed a greater percentage of AH1-specific cells that produced IFNγ and TNFα when stimulated with AH1 peptide following 15-AH1 vaccination (Fig. 6B). Examination of the phenotype of TIL from mice boosted with the AH1-peptide showed significantly less PD-1 than T cells boosted with mimotope-15 (Fig. 6C and D). Both vaccine strategies elicited cells with lower PD-1 expression than unvaccinated mice, consistent with previous reports (34). These data suggest that AH1-specific cells elicited by 15–15 vaccination can infiltrate the tumor, however, a majority of them do not functionally recognize AH1. Additionally, increased expression of PD-1 on T cells within the tumor of 15–15 vaccinated and unvaccinated mice may further contribute to functional defects observed within the tumor.

Next we determined if the 15-AH1 peptide vaccine enhanced tumor protection. Indeed, the AH1 boost significantly improved tumor-free survival (Fig. 6E). Importantly, AH1-AH1 vaccination does not result in expansion of AH1-specific cells (Fig. 1) and does not protect mice from tumor challenge (Fig. 6E) (17). Consistent with these results, T cells from the 15-AH1 vaccine kill CT26 tumor cells efficiently *in vitro* (data not shown) Therefore, in systems in which the native antigen elicits weak T cell expansion, use of mimotopes to expand cross-reactive cells followed by a native-antigen boost may better select the highest avidity and most effective tumor-specific T cells.

Discussion

For CT26, as well as in other mouse (35, 36) and human tumors (37), vaccination with native tumor antigen results in weak expansion of tumor-specific T cells. Mimotopes are one example of several vaccine strategies aimed at overcoming this problem, as mimotopes either enhance peptide-MHC binding and antigen presentation (8, 38), or alter TCR interactions (39). While mimotopes have been used effectively to expand tumor-specific T cells, it is not well understood how alterations in peptide sequence may affect the function or repertoire of the responding T cell populations (9, 10, 14). We hypothesized that boosting mimotope-elicited T cells with the native tumor-expressing antigen would select for high affinity tumor-specific T cells initially expanded by the mimotope. This hypothesis is not without precedence, as immunization with the cryptic epitope mimotope (TERT$_{572Y}$) from human telomerase followed by the native peptide (TERT$_{572R}$) resulted in higher avidity T

cell responses and a correlation with prolonged survival in patients with advanced non-small cell lung cancer (19–21, 40). Our data support and expand on these observations by using an immunodominant antigen from a mouse tumor model and a previously described poorly protective mimotope (15). After initial mimotope vaccination to activate and expand tumor-specific T cells, boosting with native antigen selects for T cells with greater affinity for tumor antigen and improves anti-tumor immunity.

Replacing the mimotope-15 boost with the AH1-peptide boost resulted in fewer AH1-specific T cells overall, but a greater frequency of 15-specific T cells that cross-reacted with the AH1 peptide. How mimotope-specific T cells that do not cross-react with the native antigen may impact AH1-specific T cell expansion or function is not yet known. One possibility is that a subsequent mimotope boost preferentially expands T cells with high affinity for the mimotope but low affinity for the tumor antigen. This possibility implies that mimotope-specific cells that do not cross-react with native peptide have increased affinity for mimotope over their cross-reactive counterparts. Competition between T cells of differing affinities is well documented, with high affinity T cells out-competing low affinity T cells specific for the same antigen (41, 42). Therefore, a heterologous boost with the native tumor antigen may remove the competition between tumor- and mimotope-specific T cells and preferentially expand mimotope-elicited cells that have high affinity for the tumor antigen.

One explanation for the decrease in number of AH1-tet+ cells observed in the 15-AH1 vaccine may be that the AH1-boost is expanding only a small population of high affinity cells. We have observed distinct differences in AH1-tet+ staining profiles with two populations of AH1-tet+ cells in mice boosted with mimotope-15, AH1-tet^{lo} and AH1-tet^{hi}. We observed lower frequencies of AH1-tet^{lo} cells in mice boosted with AH1-peptide, possibly due to AH1-tet^{hi} cells out-competing the AH1-tet^{lo} cells following vaccination. Additionally, AH1-tet^{lo} cells lost tetramer staining faster during the tetramer decay assay, indicating that these cells have lower affinity for AH1 and may not proliferate sufficiently to the AH1 boost. Therefore, the difference in cell numbers and overall relative affinity may be attributed to the absence of AH1-tet^{lo} cells in the 15-AH1 mice. Our sequencing data support that the majority of 15–15 AH1-tet^{hi} and 15-AH1 AH1-tet^{hi} sequences are shared, however their overall representation of the total sequences identified is different with the AH1-boost (Fig 5D–F, Table 1). This suggests that the AH1 boost expands cells from the AH1-tet^{hi} population, while AH1-tet^{lo} cells are not expanded.

Although the number and staining intensity of AH1-tet^{hi} cells is similar between the two vaccines, AH1-tet^{hi} cells from the 15-AH1 vaccine killed AH1-pulsed target cells more efficiently, suggesting that the two AH1-tet^{hi} populations have inherent functional differences. Furthermore, the presence of AH1-tet^{lo} cells did not inhibit AH1-tet^{hi} cells from killing AH1-pulsed targets. Further *ex vivo* clonotype analyses of 15-AH1 cells revealed preferred Vβ8.3+ usage with an enrichment in Jβ2.6 gene fragments. Previously, we identified a CDR3β motif in T cells responding to the more protective mimotopes in our model (18). This motif was found less frequently after vaccination with poorly protective mimotopes, such as mimotope-15, and was heavily selected for within AH1-tet+ cells following the heterologous AH1-boost (Fig. 5F, Table 1).

We also observed different phenotypic profiles between the AH1-specific T cells elicited by each vaccine. Most AH1-specific cells following the AH1-boost expressed KLRG-1 and down-regulated IL-7Rα, defined as short-lived effector T cells. Both SLEC and MPEC are abundant producers of cytokines and have immediate cytolytic function (31), as do the AH1-specific T cells following the AH1 boost. However, SLEC differentiation is thought to be driven by a longer duration of antigen stimulation and increased proliferation (43). Given

that AH1-tet+ cells following 15-AH1 vaccination are predominantly SLEC, the AH1 boost may be driving increased proliferation of the high avidity AH1-specific cells elicited by mimotope-15 prime. Activated effector cells have a lower ligand affinity threshold for activation than naïve T cells (44), which might explain why activated AH1-specific T cells proliferate in response to AH1 while naïve T cells do not.

Increased expression of PD-1 on activated CD8+ T cells is often an indication of functional exhaustion or anergy (45). Additionally, T cells infiltrating tumors often express high levels of PD-1, while surrounding tumor stroma expresses the PD-1 ligand, PDL-1 (34, 46). AH1-specific T cells from the spleens of the 15–15 vaccinated mice expressed high-levels of PD-1 on the day of tumor challenge compared to their AH1-boosted counterparts (Fig. 4C and D). Similarly, the TIL from mimotope-15-boosted mice expressed higher levels of PD-1, which may be associated with poor anti-tumor T cell responses observed by these lower affinity cells. It would be interesting to determine if treatment with antibodies that block PD-1/PD-1L interactions restore the function in AH1-specific T cells following 15–15 vaccination. It is not surprising that AH1-tet+ cells following 15-AH1 vaccination, being predominantly SLEC, express lower levels of PD-1. SLEC have increased levels of T-bet expression, which directly represses PD-1 expression (47). Interestingly, it has also been proposed that as competition for antigen during T cell activation increases, the level of PD-1 expression decreases, suggesting that a weaker overall activation signal may result in less PD-1 (48). If true, the AH1-boost may be delivering a weaker signal to AH1-tet+ cells compared to the boost with mimotope-15, which may still drive sufficient proliferation of the activated AH1-specific cells (44). Considering the boost vaccination occurs at the peak of the expansion phase, the AH1 boost may provide not only a sufficient signal, but also the optimal signal for these high affinity AH1-specific cells (15, 49).

Ideally, well-designed mimotopes will preferentially expand only tumor-specific cells with high avidity for the native antigen. It is important to note however that there have been reports of detectable, high avidity T cell responses to native peptide vaccines in combination with improved adjuvants. Using the unmodified self-antigen Melan-A/MART-1 and a combination of CpG oligodeoxynucleotides in Montanide, Speiser et al. demonstrated enhanced T cell function despite lower T cell frequencies when compared to vaccination with a common mimotope peptide (10). In these experiments, the 'altered peptide' vaccine elicited T cells that were less functionally reactive against the tumor. The results here support that immunization with the native antigen elicits high quality cells, although the total number or frequency may be too low to afford tumor protection. Conversely, vaccination with native-antigen in combination with mimotope vaccines may be beneficial, when immunization with the native antigen alone is insufficient.

Acknowledgments

References

1. De Visser KE, Schumacher TN, Kruisbeek AM. CD8+ T cell tolerance and cancer immunotherapy. J Immunother. 2003; 26:1–11. [PubMed: 12514424]

2. Dougan M, Dranoff G. Immune therapy for cancer. Annu Rev Immunol. 2009; 27:83–117. [PubMed: 19007331]

3. McMahan RH, Slansky JE. Mobilizing the low-avidity T cell repertoire to kill tumors. Semin Cancer Biol. 2007; 17:317–329. [PubMed: 17651986]

4. Theobald M, Biggs J, Hernandez J, Lustgarten J, Labadie C, Sherman LA. Tolerance to p53 by A2.1-restricted cytotoxic T lymphocytes. J Exp Med. 1997; 185:833–841. [PubMed: 9120389]

5. de Visser KE, Cordaro TA, Kessels HW, Tirion FH, Schumacher TN, Kruisbeek AM. Low-avidity self-specific T cells display a pronounced expansion defect that can be overcome by altered peptide ligands. J Immunol. 2001; 167:3818–3828. [PubMed: 11564799]

6. Rosenberg SA, Yang JC, Restifo NP. Cancer immunotherapy: moving beyond current vaccines. Nat Med. 2004; 10:909–915. [PubMed: 15340416]

7. Slansky JE, Rattis FM, Boyd LF, Fahmy T, Jaffee EM, Schneck JP, et al. Enhanced antigen-specific antitumor immunity with altered peptide ligands that stabilize the MHC-peptide-TCR complex. Immunity. 2000; 13:529–538. [PubMed: 11070171]

8. Parkhurst MR, Salgaller ML, Southwood S, Robbins PF, Sette A, Rosenberg SA, et al. Improved induction of melanoma-reactive CTL with peptides from the melanoma antigen gp100 modified at HLA-A*0201-binding residues. J Immunol. 1996; 157:2539–2548. [PubMed: 8805655]

9. Stuge TB, Holmes SP, Saharan S, Tuettenberg A, Roederer M, Weber JS, et al. Diversity and recognition efficiency of T cell responses to cancer. PLoS Med. 2004; 1:e28. [PubMed: 15578105]

10. Speiser DE, Baumgaertner P, Voelter V, Devevre E, Barbey C, Rufer N, et al. Unmodified self antigen triggers human CD8 T cells with stronger tumor reactivity than altered antigen. Proc Natl Acad Sci U S A. 2008; 105:3849–3854. [PubMed: 18319339]

11. Cole DK, Edwards ES, Wynn KK, Clement M, Miles JJ, Ladell K, et al. Modification of MHC anchor residues generates heteroclitic peptides that alter TCR binding and T cell recognition. J Immunol. 2010; 185:2600–2610. [PubMed: 20639478]

12. Wieckowski S, Baumgaertner P, Corthesy P, Voelter V, Romero P, Speiser DE, et al. Fine structural variations of alphabetaTCRs selected by vaccination with natural versus altered self-antigen in melanoma patients. J Immunol. 2009; 183:5397–5406. [PubMed: 19786555]

13. Adams JJ, Narayanan S, Liu B, Birnbaum ME, Kruse AC, Bowerman NA, et al. T Cell Receptor Signaling Is Limited by Docking Geometry to Peptide-Major Histocompatibility Complex. Immunity. 2011; 35:681–693. [PubMed: 22101157]

14. Iero M, Squarcina P, Romero P, Guillaume P, Scarselli E, Cerino R, et al. Low TCR avidity and lack of tumor cell recognition in CD8(+) T cells primed with the CEA-analogue CAP1-6D peptide. Cancer Immunol Immunother. 2007; 56:1979–1991. [PubMed: 17564703]

15. McMahan RH, McWilliams JA, Jordan KR, Dow SW, Wilson DB, Slansky JE. Relating TCR-peptide-MHC affinity to immunogenicity for the design of tumor vaccines. J Clin Invest. 2006; 116:2543–2551. [PubMed: 16932807]

16. Jordan KR, McMahan RH, Oh JZ, Pipeling MR, Pardoll DM, Kedl RM, et al. Baculovirus-infected insect cells expressing peptide-MHC complexes elicit protective antitumor immunity. J Immunol. 2008; 180:188–197. [PubMed: 18097019]

17. Jordan KR, McMahan RH, Kemmler CB, Kappler JW, Slansky JE. Peptide vaccines prevent tumor growth by activating T cells that respond to native tumor antigens. Proc Natl Acad Sci U S A. 2010; 107:4652–4657. [PubMed: 20133772]

18. Jordan KR, Buhrman JD, Sprague J, Moore BL, Gao D, Kappler JW, et al. TCR hypervariable regions expressed by T cells that respond to effective tumor vaccines. Cancer Immunol Immunother. 2012

19. Bolonaki I, Kotsakis A, Papadimitraki E, Aggouraki D, Konsolakis G, Vagia A, et al. Vaccination of patients with advanced non-small-cell lung cancer with an optimized cryptic human telomerase reverse transcriptase peptide. J Clin Oncol. 2007; 25:2727–2734. [PubMed: 17602077]

20. Vetsika EK, Konsolakis G, Aggouraki D, Kotsakis A, Papadimitraki E, Christou S, et al. Immunological responses in cancer patients after vaccination with the therapeutic telomerase-specific vaccine Vx-001. Cancer Immunol Immunother. 61:157–168. [PubMed: 21858533]

21. Vetsika EK, Papadimitraki E, Aggouraki D, Konsolakis G, Mela ME, Kotsakis A, et al. Sequential administration of the native TERT572 cryptic peptide enhances the immune response initiated by its optimized variant TERT(572Y) in cancer patients. J Immunother. 2011; 34:641–650. [PubMed: 21989412]

22. McWilliams JA, Sullivan RT, Jordan KR, McMahan RH, Kemmler CB, McDuffie M, et al. Age-dependent tolerance to an endogenous tumor-associated antigen. Vaccine. 2008; 26:1863–1873. [PubMed: 18329760]

23. Kemmler CB, Clambey ET, Kedl RM, Slansky JE. Elevated tumor-associated antigen expression suppresses variant Peptide vaccine responses. J Immunol. 2011; 187:4431–4439. [PubMed: 21940675]

24. Crawford F, Jordan KR, Stadinski B, Wang Y, Huseby E, Marrack P, et al. Use of baculovirus MHC/peptide display libraries to characterize T-cell receptor ligands. Immunol Rev. 2006; 210:156–170. [PubMed: 16623770]

25. Sanchez PJ, McWilliams JA, Haluszczak C, Yagita H, Kedl RM. Combined TLR/CD40 stimulation mediates potent cellular immunity by regulating dendritic cell expression of CD70 in vivo. J Immunol. 2007; 178:1564–1572. [PubMed: 17237405]

26. Fahmy TM, Bieler JG, Edidin M, Schneck JP. Increased TCR avidity after T cell activation: a mechanism for sensing low-density antigen. Immunity. 2001; 14:135–143. [PubMed: 11239446]

27. Crawford F, Kozono H, White J, Marrack P, Kappler J. Detection of antigen-specific T cells with multivalent soluble class II MHC covalent peptide complexes. Immunity. 1998; 8:675–682. [PubMed: 9655481]

28. Savage PA, Boniface JJ, Davis MM. A kinetic basis for T cell receptor repertoire selection during an immune response. Immunity. 1999; 10:485–492. [PubMed: 10229191]

29. Lee PP, Yee C, Savage PA, Fong L, Brockstedt D, Weber JS, et al. Characterization of circulating T cells specific for tumor-associated antigens in melanoma patients. Nat Med. 1999; 5:677–685. [PubMed: 10371507]

30. La Gruta NL, Doherty PC, Turner SJ. A correlation between function and selected measures of T cell avidity in influenza virus-specific CD8+ T cell responses. Eur J Immunol. 2006; 36:2951–2959. [PubMed: 17072910]

31. Lefrancois L, Obar JJ. Once a killer, always a killer: from cytotoxic T cell to memory cell. Immunol Rev. 2010; 235:206–218. [PubMed: 20536565]

32. Joshi NS, Cui W, Chandele A, Lee HK, Urso DR, Hagman J, et al. Inflammation directs memory precursor and short-lived effector CD8(+) T cell fates via the graded expression of T-bet transcription factor. Immunity. 2007; 27:281–295. [PubMed: 17723218]

33. Kaech SM, Wherry EJ. Heterogeneity and cell-fate decisions in effector and memory CD8+ T cell differentiation during viral infection. Immunity. 2007; 27:393–405. [PubMed: 17892848]

34. Ahmadzadeh M, Johnson LA, Heemskerk B, Wunderlich JR, Dudley ME, White DE, et al. Tumor antigen-specific CD8 T cells infiltrating the tumor express high levels of PD-1 and are functionally impaired. Blood. 2009; 114:1537–1544. [PubMed: 19423728]

35. McWilliams JA, McGurran SM, Dow SW, Slansky JE, Kedl RM. A modified tyrosinase-related protein 2 epitope generates high-affinity tumor-specific T cells but does not mediate therapeutic efficacy in an intradermal tumor model. J Immunol. 2006; 177:155–161. [PubMed: 16785510]

36. Ercolini AM, Ladle BH, Manning EA, Pfannenstiel LW, Armstrong TD, Machiels JP, et al. Recruitment of latent pools of high-avidity CD8(+) T cells to the antitumor immune response. J Exp Med. 2005; 201:1591–1602. [PubMed: 15883172]

37. Connerotte T, Van Pel A, Godelaine D, Tartour E, Schuler-Thurner B, Lucas S, et al. Functions of Anti-MAGE T-cells induced in melanoma patients under different vaccination modalities. Cancer Res. 2008; 68:3931–3940. [PubMed: 18483279]

38. Borbulevych OY, Baxter TK, Yu Z, Restifo NP, Baker BM. Increased immunogenicity of an anchor-modified tumor-associated antigen is due to the enhanced stability of the peptide/MHC

complex: implications for vaccine design. J Immunol. 2005; 174:4812–4820. [PubMed: 15814707]

39. Salazar E, Zaremba S, Arlen PM, Tsang KY, Schlom J. Agonist peptide from a cytotoxic t-lymphocyte epitope of human carcinoembryonic antigen stimulates production of tc1-type cytokines and increases tyrosine phosphorylation more efficiently than cognate peptide. Int J Cancer. 2000; 85:829–838. [PubMed: 10709104]

40. Kotsakis A, Vetsika EK, Christou S, Hatzidaki D, Vardakis N, Aggouraki D, et al. Clinical outcome of patients with various advanced cancer types vaccinated with an optimized cryptic human telomerase reverse transcriptase (TERT) peptide: results of an expanded phase II study. Ann Oncol. 23:442–449. [PubMed: 21873272]

41. Kedl RM, Rees WA, Hildeman DA, Schaefer B, Mitchell T, Kappler J, et al. T cells compete for access to antigen-bearing antigen-presenting cells. J Exp Med. 2000; 192:1105–1113. [PubMed: 11034600]

42. Kedl RM, Schaefer BC, Kappler JW, Marrack P. T cells down-modulate peptide-MHC complexes on APCs in vivo. Nat Immunol. 2002; 3:27–32. [PubMed: 11731800]

43. Sarkar S, Kalia V, Haining WN, Konieczny BT, Subramaniam S, Ahmed R. Functional and genomic profiling of effector CD8 T cell subsets with distinct memory fates. J Exp Med. 2008; 205:625–640. [PubMed: 18316415]

44. Kimachi K, Sugie K, Grey HM. Effector T cells have a lower ligand affinity threshold for activation than naive T cells. Int Immunol. 2003; 15:885–892. [PubMed: 12807827]

45. Ha SJ, Mueller SN, Wherry EJ, Barber DL, Aubert RD, Sharpe AH, et al. Enhancing therapeutic vaccination by blocking PD-1-mediated inhibitory signals during chronic infection. J Exp Med. 2008; 205:543–555. [PubMed: 18332181]

46. Fourcade J, Sun Z, Benallaoua M, Guillaume P, Luescher IF, Sander C, et al. Upregulation of Tim-3 and PD-1 expression is associated with tumor antigen-specific CD8+ T cell dysfunction in melanoma patients. J Exp Med. 2010; 207:2175–2186. [PubMed: 20819923]

47. Kao C, Oestreich KJ, Paley MA, Crawford A, Angelosanto JM, Ali MA, et al. Transcription factor T-bet represses expression of the inhibitory receptor PD-1 and sustains virus-specific CD8+ T cell responses during chronic infection. Nat Immunol. 12:663–671. [PubMed: 21623380]

48. Obar JJ, Lefrancois L. Early signals during CD8 T cell priming regulate the generation of central memory cells. J Immunol. 2010; 185:263–272. [PubMed: 20519649]

49. Slansky JE, Jordan KR. The Goldilocks model for TCR-too much attraction might not be best for vaccine design. PLoS Biol. 8:1–4.
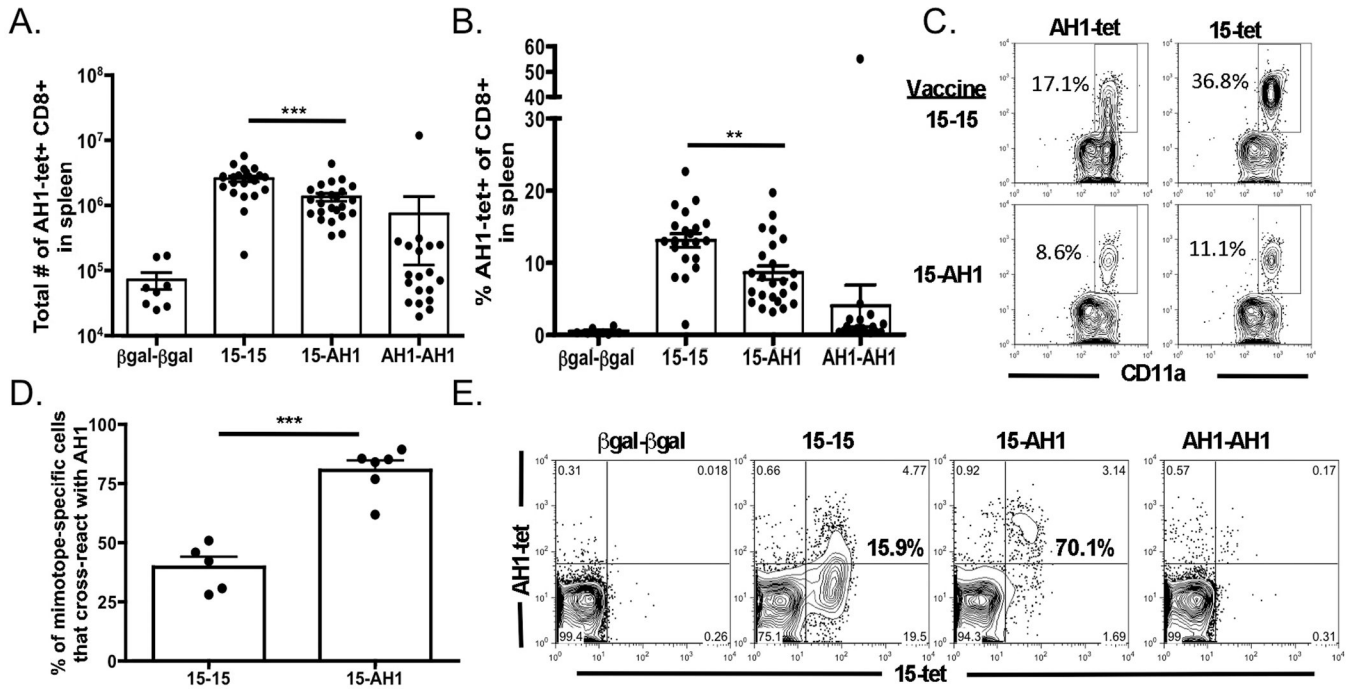
Figure 1. Higher frequency of T cells that cross-react with the AH1 antigen following the 15-AH1 vaccine, despite no increase in total AH1-specific T cells

Mice were vaccinated as described and splenocytes were analyzed by flow cytometry for AH1-tet+CD8+ T cells 7 days following boost. A) Total number and B) frequency of AH1-tet+CD8+ Dump- T cells in the spleen 7 days after the boost are shown respectively (*** p = 0.0003,** p = 0.0076). Figures depict five combined experiments with 4–5 mice per experiment. C) Splenocytes from vaccinated mice were stained with either AH1-tet or 15-tet. D) The frequency of 15-tet+CD8+ T cells that cross-react with AH1-tet was derived from the plots in (C) (*** p < 0.0001). E) Representative plots of splenocytes co-labeled with AH1-tet-PE and 15-tet-AF647. Bold percentages reflect the frequency of 15-tet+ cells that cross-react with AH1-tet.
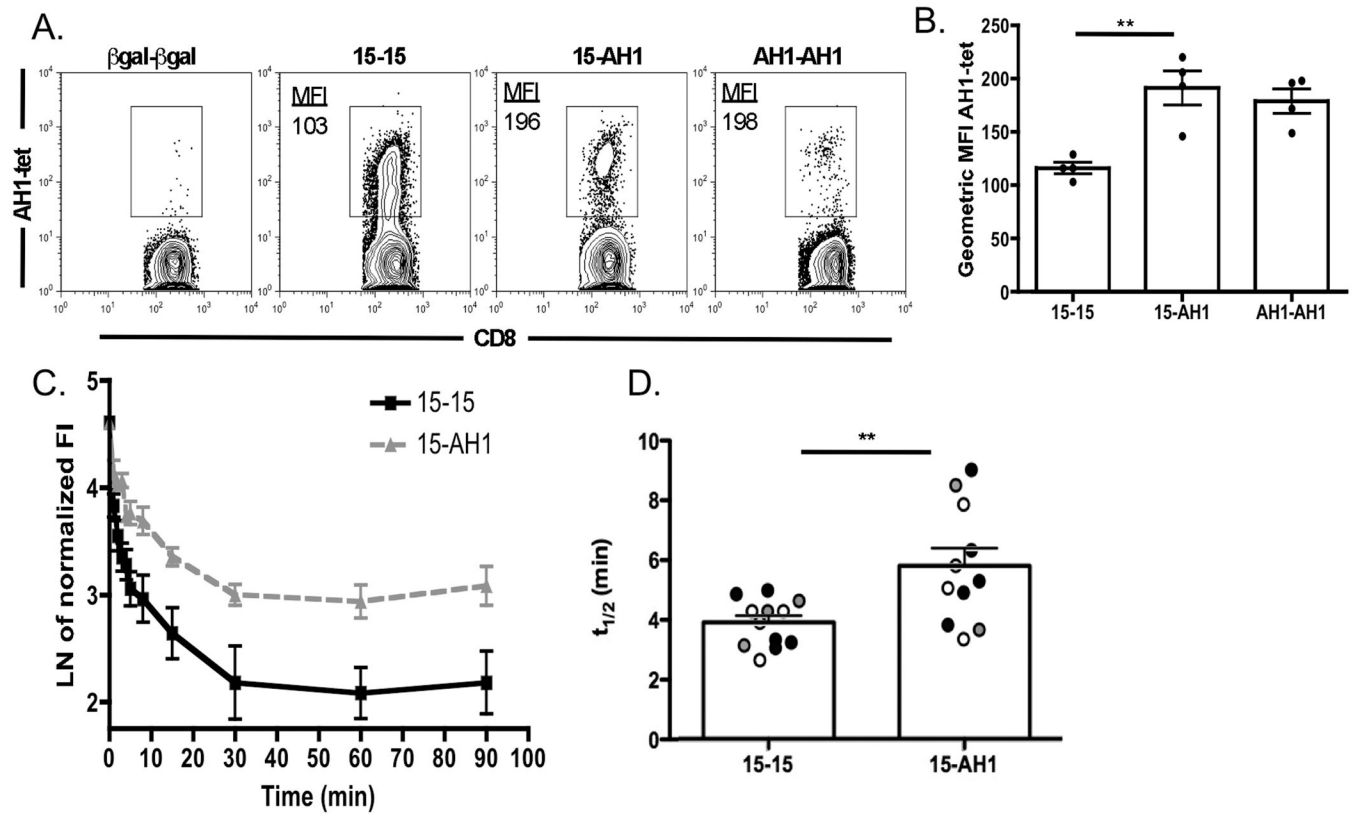
Figure 2. AH1-specific T cells following AH1-boost have increased affinity for AH1-tetramer
A) Mice were immunized as in Figure 1 and AH1-tet+ T cells were analyzed by flow cytometry. B) AH1-tet+ T cells were analyzed as in A, and the geometric MFI was determined. Symbols represent individual mice and data reflect one of five independent experiments (** p = 0.0068) with similar results. C) Splenocytes from 15–15 (■) or 15-AH1 (▲) vaccinated mice were stained with AH1-tet and used in a tetramer decay assay. D) Half-life of tetramer decay from (C) was determined from a one-phase exponential decay curve. Each symbol represents an individual mouse and different colors represent three independent experiments (** p = 0.0054).
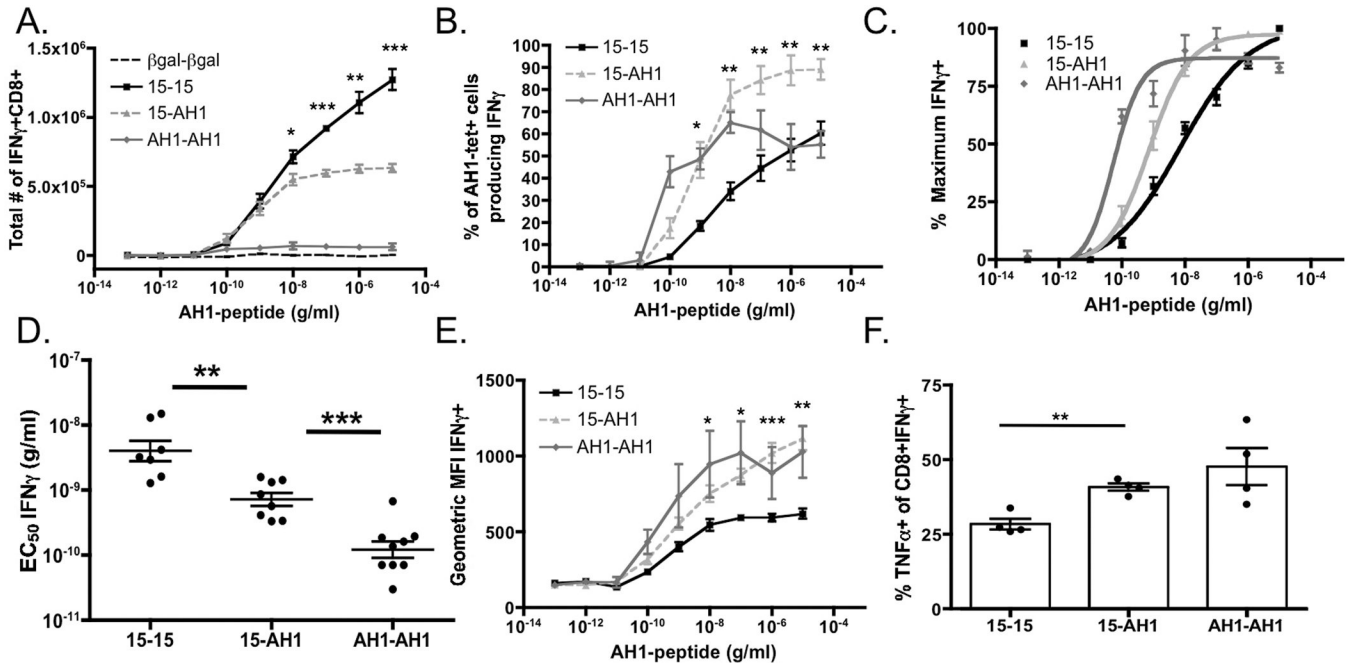
Figure 3. AH1-specific T cells from AH1-boosted mice have increased functional avidity for AH1 and a greater frequency produce multiple cytokines

Mice were vaccinated as in Figure 1 and splenocytes were stimulated *ex vivo* with AH1 peptide. Splenocytes from 15–15 (■, solid), 15-AH1 (▲, dashed), AH1-AH1 (◆, solid) or βgal-βgal (black, dashed) were stained for CD8+ T cells and intracellular cytokine as indicated. A) The total number of IFNγ+CD8+ T cells in the spleen is shown. B) Plot represents IFNγ + cells as a frequency of AH1-tet+ cells. C) Plot represents percent maximum of IFNγ production at highest peptide concentration. Points were fit to a nonlinear sigmoidal dose response curve and D) EC$_{50}$ values were calculated. Plot combines two individual experiments with 4–5 mice per group. E) Geometric MFI of IFNγ over the range of AH1-peptide stimulation gated on total IFNγ+ cells. F) Frequency of TNFα+ of IFNγ+CD8+ (** p = 0.0013). All statistics compare 15–15 vs. 15-AH1 unless specifically noted (*** p 0.0005, ** p 0.005, * p 0.05).
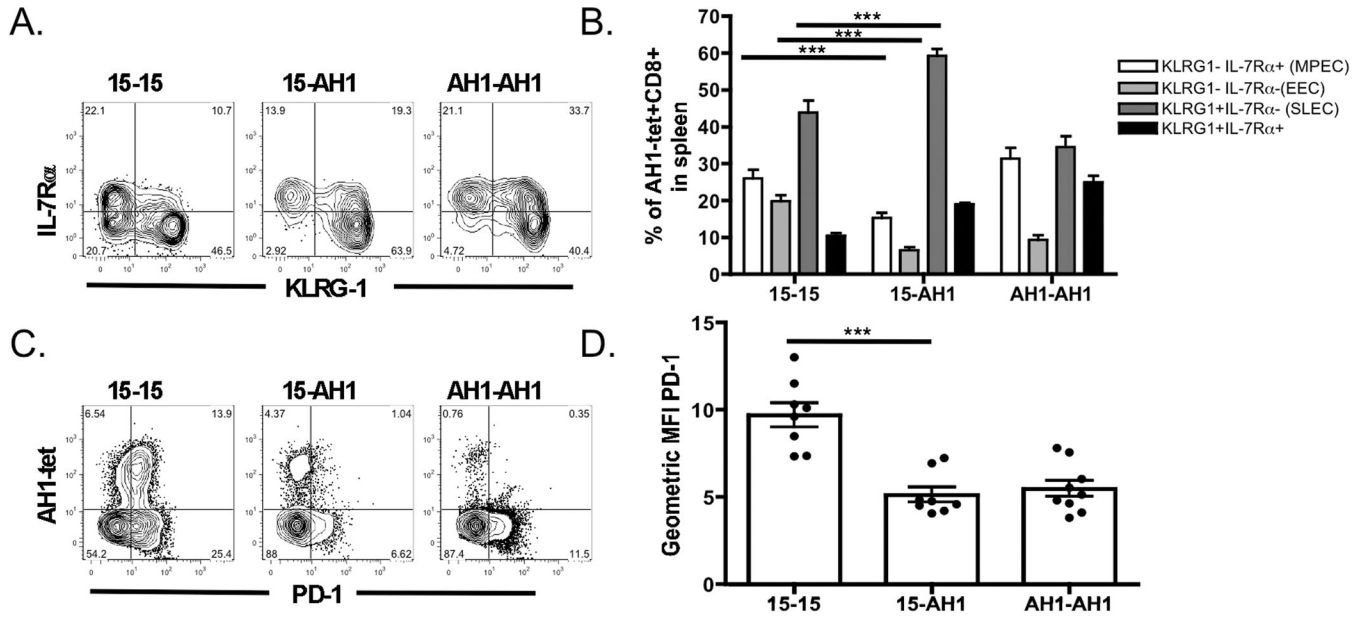
Figure 4. The AH1-boost elicits 'short-lived' effector cells with decreased PD-1 expression
A) Mice were vaccinated as in Figure 1 and splenic CD8+Dump-AH1-tet+ cells were assessed for expression of KLRG-1 and IL-7Rα. B) Frequency of each group of cells from (A) in the AH1-tet+ gate is shown (□ KLRG-1-IL-7Rα+, ▨ KLRG-1-IL-7Rα-, ▦ KLRG-1+IL-7Rα-, ■ KLRG-1+IL-7Rα+). Data represent one of five individual experiments with 4–5 mice per group (*** p < 0.0001). C) AH1-tet+ splenocytes were stained *ex vivo* for PD-1 expression and D) the geometric MFI of PD-1 expression on AH1-tet+ cells was plotted (*** p = < 0.0001).
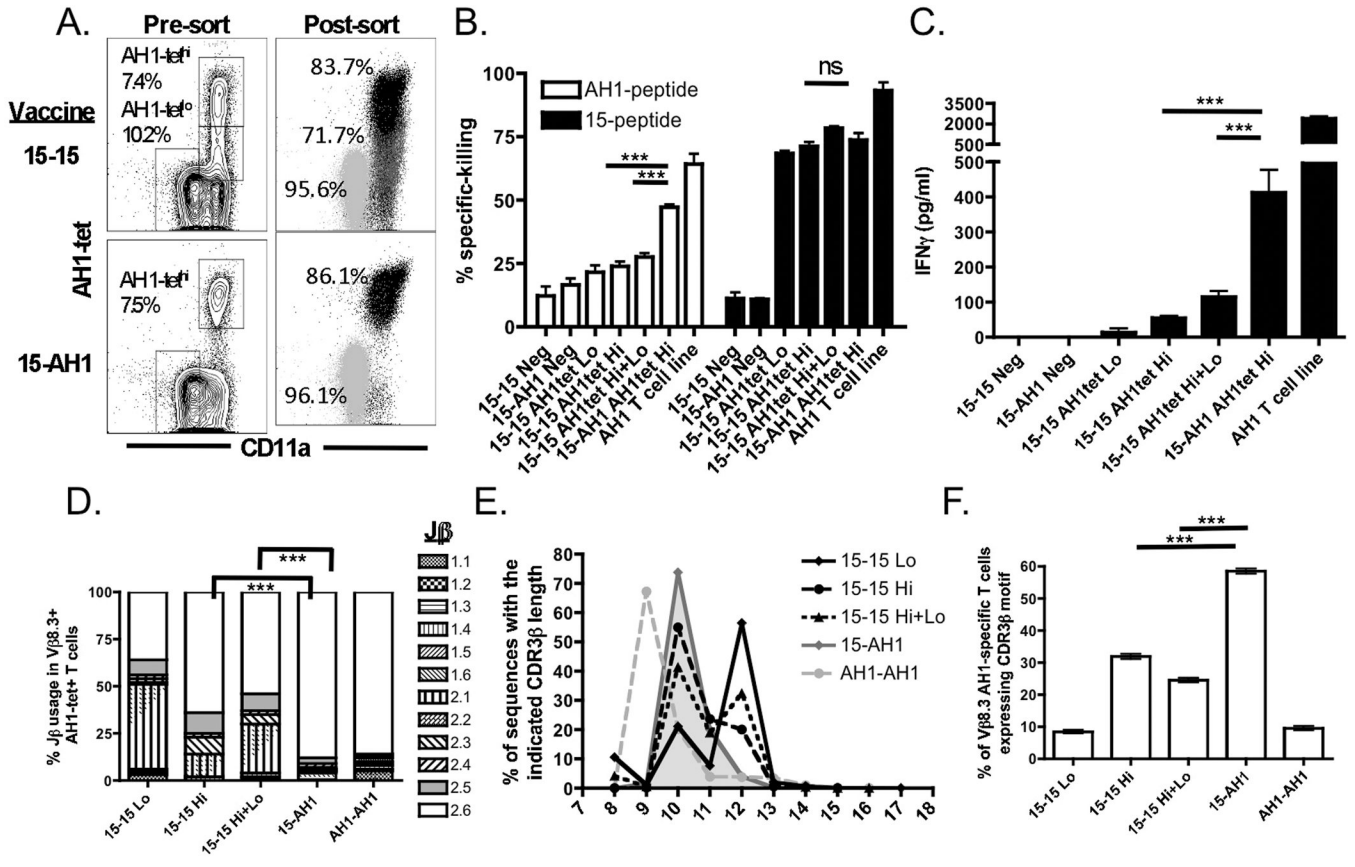
Figure 5. The AH1-specific T cell repertoire from mice that received the AH1 boost differs and have enhanced reactivity against the AH1 antigen

A) AH1-tet+ cells were sorted as indicated. Pre- and post-sort analyses of AH1-tet+ T cells are shown. B) Sorted AH1-tet^{hi} cells were incubated with CFSE-labeled peptide-pulsed target cells for 12 h and percent specific killing of target cells loaded with AH1 peptide (□) or mimotope-15 peptide (■) was determined. Data shown are from one of two representative experiments with assay run in triplicate (*** p < 0.0001). C) Supernatant from the killing assay was collected and IFNγ production was determined by ELISA (*** p < 0.0001). D) cDNA from sorted AH1-tet+ cells was sequenced using Vβ8-specific primers. The frequency of Vβ8.3+ sequences expressing different Jβ-regions is shown. The frequency of Jβ2.6+ was compared using a difference in proportions test and generating chi square values at a 95% confidence level (*** p < 0.0001). E) The amino acid length of the CDR3β-region is plotted as a frequency of Vβ8.3+ sequences (◆ 15–15 Lo, ● 15–15 Hi, ▲ 15–15 Total, ◆ 15-AH1 (filled), ● AH1-AH1). F) The frequency of Vβ8.3+ sequences expressing the CDR3β motif in each vaccine cohort is shown. Error bars represent 95% confidence intervals (*** p < 0.0001).
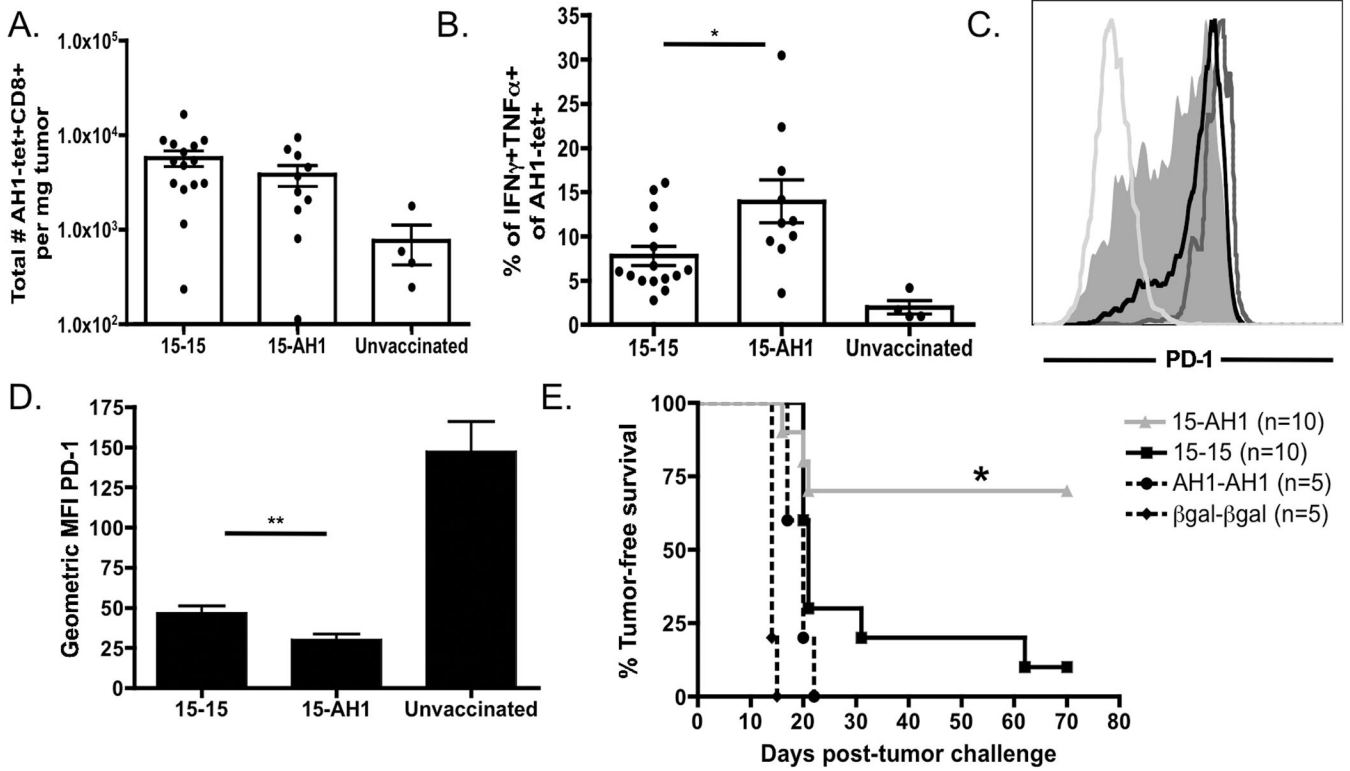
Figure 6. Boosting with the native tumor antigen improves TIL function and enhances anti-tumor immunity

A) Mice were vaccinated as described in Figure 1 and challenged with CT26 1 day following the boost. A) The total number of infiltrating AH1-tet+CD8+ T cells per mg of tumor was determined. Data are compiled from four individual experiments with 2–4 mice per group. B) TIL were isolated, stimulated with 10 μg/ml AH1-peptide, and analyzed for intracellular IFNγ and TNFα. Plot represents the percentage of AH1-tet+ cells producing both cytokines. Data from four experiments are combined (* p = 0.0164). C) Histograms showing PD-1 expression gated on AH1-tet+CD8+Dump- cells from 15–15 (— unfilled) 15-AH1 (— filled), unvaccinated (— unfilled), and negative spleen control (— unfilled). D) Data from (C) were combined and expression levels of PD-1 are shown (** p < 0.05). E) Mice were vaccinated as in Figure 1 with 15–15 (■), 15-AH1(▲), AH1-AH1 (●), or βgal-βgal (◆) and challenged with CT26 tumor cells seven days following the second vaccination (day 0). Tumor growth was monitored and mice were sacrificed when tumors reached 100 mm^2 (* p = 0.016, 15-AH1 compared to 15–15).

Table 1

The most frequent Vβ8.3 TCR sequences identified following the AH1 boost are elicited by the mimotope-15 vaccine at lower frequency.

Jβ-Region	Codons[a]	CDR3β Region[b] (V+Random+J)	CDR3β Motif	% of 15-AH1 (n=22254)	% of 15-15 Hi+Lo (n=24353)	% of 15-15 Hi (n=22625)	% of 15-15 Lo (n=22805)	% of AH1-AH1 (n=22592)
Jβ 2.6	11	cASSDGDYEQYf	+	12.96	6.76	10.29	1.40	1.18
Jβ 2.6	9	cASSDGHYEQYf	+	10.28	0.90	1.68	0.13	-
Jβ 2.6	11	cASSDGLGYEQYf		5.90	1.04	0.91	0.36	-
Jβ 2.6	1	cASSPGSYEQYf	+	3.05	-	-	-	-
Jβ 2.6	4	cASSDGRYEQYf	+	2.88	0.51	0.39	0.01	-
Jβ 1.3	2	cASSEGQGNTLYf		2.16	0.01	-	-	-
Jβ 2.6	9	cASSEGSYEQYf	+	1.85	0.35	0.85	0.06	-
Jβ 2.6	2	cASGQGDYEQYf		1.75	-	0.03	-	-
Jβ 2.6	6	cASSEGQYEQYf	+	1.71	0.77	1.00	0.27	0.27
Jβ 2.6	8	cASSDGQYEQYf	+	1.56	0.79	1.37	0.22	0.97
Jβ 2.6	7	cASSDGSYEQYf	+	1.29	0.03	0.09	-	-
Jβ 2.4	3	cASSEGQGNTLYf[c]		1.23	0.01	-	-	-
Jβ 2.5	1	cASSERLGQDTQYf		1.23	0.60	1.32	0.09	-
Jβ 2.6	2	cASSQGAYEQYf		1.13	0.02	0.02	-	-
Jβ 2.6	2	cASSDGTGYEQYf		1.08	4.40	7.33	0.82	-
Jβ 2.6	1	cASSEGVYEQYf		0.98	0.03	0.10	-	-
Jβ 2.6	1	cASSAGSYEQYf	+	0.91	0.02	-	-	-
Jβ 2.6	3	cATGTGAYEQYf		0.85	-	0.05	-	-
Jβ 2.6	1	cASSGGTNYEQYf		0.77	-	-	-	-
Jβ 2.6	1	cAAGTGAYEQYf		0.65	0.07	-	-	0.02
Jβ 2.6	4	cASSDGAYEQYf		0.62	0.13	0.34	0.03	-
Jβ 2.6	4	cASSEGHYEQYf	+	0.53	2.42	2.05	1.75	-
Jβ 2.5	1	cASSDLLGQDTQYf		0.50	-	-	-	-

Jβ-Region	Codons[a]	CDR3β Region[b] (V+Random+J)	CDR3β Motif	% of 15-AH1 (n=22254)	% of 15-15 Hi+Lo (n=24353)	% of 15-15 Hi (n=22625)	% of 15-15 Lo (n=28805)	% of AH1-AH1 (n=22592)
Jβ 2.6	4	cASS**EGK**YEQYf	+	*0.45*	-	-	-	0.01
Jβ 2.6	1	cASSD**K**YEQYf		*0.41*	0.05	0.02	-	-
Jβ 2.6	1	cASSD**GWGQ**EQYf		*0.41*	-	-	-	-
Jβ 2.6	1	cASS**TGA**YEQYf	+	*0.40*	-	0.01	-	0.01
Jβ 2.6	2	cASS**EGR**YEQYf	+	0.33	*0.94*	0.92	0.11	-
Jβ 2.1	1	cASSD**GDA**EQFf	-	0.31	-	-	-	-
Jβ 2.6	2	cASSD**GT**YEQYf	+	*0.31*	0.07	0.22	-	0.10

[a]Total number of codons identified refers to the number of unique DNA sequences identified for each CDR3β

[b]Amino acids between V and J regions are in bold

[c]Identical amino acid sequences identified in 15-15 using a different Jβ-region

Dark grey rows indicate sequences from 15-AH1 that were not identified in either 15-15 or AH1-AH1 vaccines

Light grey rows indicate sequences from 15-AH1 unique to the AH1-AH1 vaccine

Bold numbers indicate the highest observed representation of total sequences for each CDR3β